

---

# Benchmarking Unlearning for Vision Transformers

---

Kairan Zhao<sup>\*1</sup> Iurie Luca<sup>\*1</sup> Peter Triantafillou<sup>1</sup>

## Abstract

Research in machine unlearning (MU) has gained strong momentum: MU is now widely regarded as a critical capability for building safe and fair AI. In parallel, research into transformer architectures for computer vision tasks has been highly successful: Increasingly, Vision Transformers (VTs) emerge as strong alternatives to CNNs. Yet, MU research for vision tasks has largely centered on CNNs, not VTs. While benchmarking MU efforts have addressed LLMs, diffusion models, and CNNs, none exist for VTs. *This work is the first to attempt this, benchmarking MU algorithm performance in different VT families (ViT and Swin-T) and at different capacities.* The work employs (i) different datasets, selected to assess the impacts of dataset scale and complexity; (ii) different MU algorithms, selected to represent fundamentally different approaches for MU; and (iii) both single-shot and continual unlearning protocols. Additionally, it focuses on benchmarking MU algorithms that leverage training data memorization, since leveraging memorization has been recently discovered to significantly improve the performance of previously SOTA algorithms. En route, the work characterizes how VTs memorize training data relative to CNNs, and assesses the impact of different memorization proxies on performance. The benchmark uses unified evaluation metrics that capture two complementary notions of forget quality along with accuracy on unseen (test) data and on retained data. Overall, this work offers a benchmarking basis, enabling reproducible, fair, and comprehensive comparisons of existing (and future) MU algorithms on VTs. And, for the first time, it sheds light on how well existing algorithms work in VT settings, establishing a promising reference performance baseline.

## 1. Introduction

The high success of Vision Transformers (VTs) brings with it new responsibilities regarding responsible/fair/safe AI. Among these, the ability to remove (the influence of) specific “problematic” data from trained models (a.k.a. machine unlearning) (MU) is critical. Said problematic data may include biased, erroneous, poisoned, obsolete, or privacy-sensitive data. Popular VT architectures represent thus an important frontier in this challenge. On the other hand, recently memorization has been identified as playing a fundamental role for MU (and this holds across modalities). For instance, MU research in LLMs (Barbulescu and Triantafillou, 2024; Jang et al., 2022) and in diffusion models (Ren et al., 2024; Wen et al., 2024) explicitly detects and mitigates memorization. In computer-vision tasks, memorization has been shown to be a key factor affecting unlearning performance (Zhao et al., 2024; Torkezadehmahani et al., 2024).

Despite the fact that memorization and MU have been extensively studied in LLMs, text-to-image Diffusion Models, and Convolutional Networks (CNNs), it is an open question whether findings transfer to VTs. This uncertainty stems from key differences in architecture, training regimes, and inductive biases. Compared to LLMs (with which they share a transformer backbone), VTs operate on image patches using global self-attention (unlike LLMs which rely on causal masking or token-order constraints and process semantically meaningful tokens) and VTs are typically (pre)trained using supervised classification objectives (e.g., on ImageNet), while LLMs are trained on large corpora using self-supervised objectives, yielding different types of data exposure and memorization. Compared to CNNs, VTs lack strong spatial inductive biases such as locality (semantically related neighbouring pixels), translation equivariance (for positional reasoning). These biases help CNNs localize and isolate memorization effects, whereas VTs must learn such structure from data alone, making VTs more data-hungry, often necessitating a pretrain–then–finetune training regime. Moreover, unlike LLMs, VTs lack the benefit of language’s syntactic and semantic structure. Hence, learned representations are more entangled and spread across layers and attention heads.

**The Gap.** One can thus reasonably expect the above dif-

---

<sup>1</sup>University of Warwick, United Kingdom. Correspondence to: Kairan Zhao <Kairan.Zhao@warwick.ac.uk>.

Preprint. February 24, 2026.

ferences to collectively introduce unique challenges for unlearning in VTs. Said potential challenges remain largely unexplored, despite a few related research works on both the algorithmic side (e.g., Cadet et al. (2024); Cho et al. (2024) whose evaluations of CNN-derived unlearning also include some VT, typically, ViT-Tiny) and on the benchmarking side, with recent efforts systematically evaluating MU across tasks and modalities (such as Maini et al. (2024); Li et al. (2024) for LLMs, Ma et al. (2024); Zhang et al. (2024), and Cheng and Amiri (2024) for text-to-image diffusion models).

Focusing on vision, image classification tasks, the first comprehensive attempt in this domain, by Triantafillou et al. (2024), was based on the NeurIPS 2023 MU competition, evaluating and ranking the top algorithms on two datasets from the competition on a CNN (ResNet-18) architecture. Interestingly, they report that MU methods can be brittle across architectures/datasets. Grimes et al. (2024) benchmarked MU on the same CNN environment but focused on evaluating more demanding privacy threats and paid attention to continual MU. Cadet et al. (2024) extended the benchmark in Triantafillou et al. (2024), evaluating 18 MU algorithms on four datasets on a ResNet (as well as on ViT-Tiny). Each of the above benchmarks has a different emphasis: Each is typically designed for a specific architecture-modality-task pairing. Some stress new datasets, while others stress comprehensive/exhaustive examinations/rankings of a large set of MU algorithms.

**This work.** Overall, benchmarking for MU has been addressed for LLMs, diffusion models, and CNNs, but not for VTs. We fill this gap by benchmarking MU on VTs, contributing an evaluation basis along the following key axes:

1. **Memorization:** Do VTs memorize differently to CNNs? How does this affect unlearning?
2. **Proxies:** Are CNN-based memorization proxies effective in VTs? Can they improve unlearning?
3. **Algorithms:** How do fundamentally different approaches for CNN-based MU perform on VTs?
4. **VT architectures:** Do VTs design choices (ViT vs. Swin-T) and *capacity* impact unlearning?
5. **Pretrain–Finetune:** How does the VTs’ pretrain–finetune paradigm influence MU?
6. **Algorithm–Architecture Pairings:** Are certain pairings especially compatible?
7. **Continual MU on VTs:** How stable is performance under continual unlearning?

In contrast to prior “standard” benchmarking research which are leaderboard-style (benchmarking/ranking a large set of algorithms) or proposing new datasets, our work follows a different path: It is centered on VTs, systematically testing *representative* MU approaches across *two* VT families (ViT, Swin-T) at *different* capacities each, over *four*

datasets of varying size/complexity, and under *both* single-shot and continual unlearning scenarios. We employ unified metrics (ToW, ToW-MIA) that jointly account for retain/test accuracy, forget accuracy, and MIA vulnerability. We contrast results against CNN-derived MU counterpart algorithms. We aim to isolate architecture, capacity, memorization (and proxy) effects to assess how well MU methods perform in VTs and establish a strong performance baseline regarding MU performance in VTs. The code for reproducing the results is available at: [https://github.com/kairanzhao/Unlearning\\_VTs](https://github.com/kairanzhao/Unlearning_VTs)

## 2. Model Architectures and Algorithms

### 2.1. Vision Transformers

Transformer architectures (Vaswani et al., 2017) leverage self-attention mechanisms instead of recurrence. We focus on, arguably, the two most popular VTs: ViT and Swin-T. ViT (Dosovitskiy et al., 2021) processes images as sequences of flattened, embedded patches, which are (i) projected into an embedding space, (ii) combined with positional encodings, and (iii) passed through transformer encoder layers comprising multi-headed self-attention (MSA) and multi-layer perceptrons (MLP). Swin-T (Liu et al., 2021) adds hierarchical representations (à la CNNs) by progressively merging patches and reducing spatial resolution at deeper layers, forming multi-scale representations. Additionally, a shifted-window self-attention mechanism is introduced to model both local and global contexts. These allow us to study MU performance on architectures which, due to having/lacking hierarchical representations, are more/less similar to CNNs (Swin-T/ViT).

### 2.2. Machine Unlearning (MU)

MU (Cao and Yang, 2015) aims to remove the influence of specific (“problematic”) training examples from pretrained models. A large body of work has tackled MU, spanning formal definitions and guarantees (Ginart et al., 2019; Sekhari et al., 2021; Neel et al., 2020), empirically effective methods (Goel et al., 2022; Golatkar et al., 2020; Thudi et al., 2022), and other earlier efforts (Xu et al., 2023). Over time, several key baselines have emerged, capturing fundamental components for successful MU. These range from simpler baselines like Fine-tune (FT) (Warnecke et al., 2023; Golatkar et al., 2020), to more sophisticated baselines like NegGrad+ (Kurmanji et al., 2023). Most recent SOTA algorithms include SCRUB (Kurmanji et al., 2023), L1-sparse (Jia et al., 2024), Salun (Fan et al., 2024) and the meta-algorithmic framework RUM (Zhao et al., 2024).

Evidently, all of the above methods have focused on CNNs. Our contributions aim to answer whether the above CNN-derived, MU algorithms transfer to VTs across VT fami-

lies, model capacities, datasets, and protocols. Our benchmark offers a substrate where such existing and new methods and architectures can be integrated and systematically evaluated.

Following prior MU work (Kurmanji et al., 2023; Fan et al., 2024), we select three representative families of MU methods, which capture distinct unlearning paradigms and are commonly used as baselines in the literature: (i) FT, a standard baseline that fine-tunes the model on retained data only and is typically effective for low-memorization examples; (ii) NegGrad+, a strong gradient-based baseline that explicitly promotes forgetting by pushing model parameters away from the forget set while preserving performance on retained data; and (iii) SalUn, a recent SOTA that performs parameter-selective unlearning based on saliency.

All MU methods assume a training dataset  $D$  partitioned into a forget set  $D_f$  and a retain set  $D_r = D \setminus D_f$ . FT continues training exclusively on  $D_r$ . NegGrad+ combines standard fine-tuning on  $D_r$  with gradient ascent on  $D_f$ , aiming to balance retention and forgetting simultaneously during unlearning. SalUn first identifies the key parameters influencing examples in  $D_f$  using a saliency criterion, and then updates only these parameters while perturbing the associated labels of examples in  $D_f$ .

In addition to comparing raw instantiations of these methods, we instantiate all three within the RUM framework, which has been shown to consistently strengthen a wide range of MU algorithms (Zhao et al., 2024). This allows us to compare method families under their best-performing configurations.

### 2.3. Leveraging Memorization for Unlearning

Memorization quantifies model dependency on specific examples (Feldman, 2019; Feldman and Zhang, 2020). Let  $D_{-i} := D \setminus (x_i, y_i)$  and  $\Pr_{D}[\cdot] := \Pr_{f \sim A(D)}[\cdot]$ , the measure, referred to as *memorization score*, is defined as

$$\text{mem}(A, D, i) = \Pr_D[f(x_i) = y_i] - \Pr_{D_{-i}}[f(x_i) = y_i], \quad (1)$$

capturing how predictions change when removing an example from training. Robust computation of this metric necessitates training large number of models (each retrained on subsets excluding specific examples) to achieve stable estimates, which is especially expensive, particularly for VTs. Proxies like the four *Learning Events Proxies* (Confidence (Conf), Max Confidence (MaxConf), Entropy (Ent), and Binary Accuracy (BA)) (Jiang et al., 2021) and *Hold-out Retraining (HR)* (Carlini et al., 2019) come to the rescue, efficiently estimating memorization scores. The formulas for each of these can be found in the Appendix A.3.

RUM leverages memorization to improve unlearning performance. It is structured in three stages: (1) *Refinement*:

Partitions the forget set into homogeneous subsets based on memorization scores of examples in the forget set. Specifically, it creates three partitions consisting of low-, medium- and highly-memorized forget examples. (2) *Matching*: Selects suitable unlearning methods tailored to each partition. (3) *Unlearning*: Applies an unlearning algorithm sequentially on the three partitions.

We evaluate FT, NegGrad+, and SalUn within the RUM framework. Concretely, RUM applies each base unlearning method sequentially to the three memorization-based partitions (e.g., RUM(SalUn)). For simplicity, we refer to these instantiations as SalUn, NegGrad+, and FT, respectively. We adopt this evaluation protocol because instantiating MU algorithms within RUM has been shown to substantially strengthen their performance (Zhao et al., 2024). For completeness, we additionally demonstrate in Section A.4 in Appendix that this improvement over vanilla instantiations also holds for Vision Transformers.

## 3. Experimental Setup

### 3.1. Data Sets

We evaluate unlearning methods on four different image classification benchmarks that vary in dataset size, semantic complexity, and number of classes. Specifically, we use CIFAR-10, CIFAR-100 (Krizhevsky, 2009), and SVHN (Netzer et al., 2011), which are standard datasets commonly adopted in prior machine unlearning studies. To assess scalability to larger and more complex settings, we additionally benchmark on ImageNet-1K (Deng et al., 2009) using its validation set. Among these, CIFAR-10 and CIFAR-100 provide controlled settings with increasing class granularity, while SVHN represents a large-scale but semantically simpler dataset. ImageNet-1K serves as the pretraining dataset for VTs and enables evaluation under realistic, high-complexity conditions.

### 3.2. Transformer Architectures and Implementations

We focus on ViT and Swin variants with model sizes comparable to ResNet-50 to enable fair comparisons with CNN-based unlearning results. Our primary benchmarks are ViT-Small and Swin-Tiny, which have similar parameter counts but differ substantially in inductive biases: ViT relies on global self-attention, whereas Swin introduces hierarchical structure and locality through windowed attention.

To study the effect of model capacity, we additionally evaluate smaller and larger variants, including ViT-Tiny, ViT-Base, Swin-Small, and Swin-Base. This allows us to examine whether unlearning behavior varies systematically with model scale and architectural bias.

### 3.3. Evaluation Metrics

**Unlearning Metrics.** The unlearned model  $\theta_u = U(\theta_o, D_f, D_r)$  must balance forgetting quality (on  $D_f$ ) while preserving model performance (on  $D_r$ ) and generalizing well to unseen test data  $D_{test}$ . We adopt two primary metrics from Zhao et al. (2024) to assess this balance. ToW( $\theta_u, \theta_r, D_f, D_r, D_{test}$ ) (ToW for short):

$$\text{ToW} = (1 - \Delta a(\theta_u, \theta_r, D_f)) \cdot (1 - \Delta a(\theta_u, \theta_r, D_r)) \cdot (1 - \Delta a(\theta_u, \theta_r, D_{test})) \quad (2)$$

where  $a(\theta, D) = \frac{1}{|D|} \sum_{(x,y) \in D} \mathbb{1}[f(x; \theta) = y]$  is the accuracy of a model  $f$  parametrized by  $\theta$  on  $D$ , and  $\Delta a(\theta_u, \theta_r, D) = |a(\theta_u, D) - a(\theta_r, D)|$  is the absolute difference in accuracy between  $\theta_u$  and the retrained-from-scratch model  $\theta_r$  on  $D$ . And, ToW-MIA( $\theta_u, \theta_r, D_f, D_r, D_{test}$ ) (ToW-MIA):

$$\text{ToW-MIA} = (1 - \Delta m(\theta_u, \theta_r, D_f)) \cdot (1 - \Delta a(\theta_u, \theta_r, D_r)) \cdot (1 - \Delta a(\theta_u, \theta_r, D_{test})) \quad (3)$$

where  $m(\theta, D) = \frac{TN_D}{|D|}$  and  $\Delta m(\theta_u, \theta_r, D) = |m(\theta_u, D) - m(\theta_r, D)|$ . In ToW-MIA,  $m(\theta, D)$  accounts for “forget quality” using Membership Inference Attack (MIA) performance. To calculate this, as in Fan et al. (2024); Zhao et al. (2024); Jia et al. (2023), we train a binary classifier  $C$  that classifies examples as “in-training” or “out-of-training”. We simplify our notation  $l(f(x; \theta), y)$  (the cross-entropy loss of a model with weights  $\theta$  on example  $x$  with label  $y$ ) to  $l(x, y)$ .  $C$  is trained on loss values from a balanced dataset  $D_t^b = \{l(x_i, y_i), y_i^b\}$ , where examples  $x_i$  are drawn equally from the retain set  $D_r$  (labelled as  $y_i^b = 1$  for “training”) and the test set  $D_{test}$  (labelled as  $y_i^b = 0$  for “non-training”). Once trained,  $C$  evaluates loss values for examples in  $D_f$ .  $m(\theta, D)$  measures the proportion of  $D_f$  examples that  $C$  classified as “non-training”, i.e. the true negatives  $TN_D$ . The hope is for the unlearning method to cause the model to treat forget set examples as if they were never seen during training, resulting in the classifier categorising them as “non-training.” So similarly to  $\Delta a$ ,  $\Delta m(\theta_u, \theta_r, D)$  quantifies how closely the unlearned model  $\theta_u$  resembles the MIA performance of the retrain-from-scratch model  $\theta_r$ .

ToW and ToW-MIA measure “forget quality” differently: ToW uses accuracy differences on the forget set, while ToW-MIA uses differences in MIA vulnerability. Both range from 0 to 1, with higher values indicating better unlearning performance (closer-matching retraining from scratch). Together, ToW and ToW-MIA provide a comprehensive view of unlearning performance.

**Memorization Proxy Metric.** To evaluate how well a proxy captures memorization, we compute Spearman’s rank correlation coefficient between the ground-truth mem-

orization score and the proxy value across training examples. For each example  $(x_i, y_i) \in D$ , let  $m_i = \text{mem}_m(A, D, i)$  denote the “Feldman” memorization score (Feldman, 2019) and  $p_i = \text{proxy}(x_i, y_i)$  the value of a given proxy metric. We rank  $m_i$  and  $p_i$  independently and compute Spearman’s  $\rho$  between their ranks. The resulting coefficient  $\rho \in [-1, 1]$  measures the strength and direction of the monotonic relationship between true memorization and the proxy, with larger absolute values indicating stronger correlation.

## 4. Results and Analyses

In this section we present the main results, focusing on CIFAR-100 as a representative dataset. The Appendix contains results for the other datasets. Also, as we focus on memorization-based MU algorithms, we first established that (i) the memorization patterns in VTs mimic those in CNNs and that (ii) memorization proxies can indeed be trustworthy for being leveraged by MU algorithms in VTs. The detailed results can be found in Appendix A.3.

### 4.1. Memorization and Proxies in VTs

Memorization plays a central role in unlearning, so we first ask whether VTs memorize similarly to CNNs, and whether CNN-derived proxies remain valid predictors of memorization in VTs.

**Key Takeaways–Memorization patterns.** We observe (see Figure 3, 4 in Appendix A.3.1) the same long-tailed distributions previously reported for CNNs (Feldman and Zhang, 2020). Thus, VTs and CNNs display fundamentally similar memorization behavior, despite architectural differences. Also, on CIFAR-10, VTs exhibit slightly lower memorization than ResNet-18, reflecting their ability (via pretraining and global attention) to rely less on memorizing individual examples for simpler tasks.

**Key Takeaways–Proxy validity.** Whether CNN-derived proxies remain valid for VTs is unclear due to differences in their inductive biases and training regimes. We evaluated five memorization proxies: Confidence (Conf), Max Confidence (MaxConf), Entropy (Ent), Binary Accuracy (BA) (Jiang et al., 2021), and Holdout Retraining (HR) (Carlini et al., 2019). The results are in Table 1.

The Confidence proxy consistently achieves the strongest correlations across all models and datasets, with magnitudes (-0.79 to -0.91) closely resembling those in CNNs. Swin-Tiny shows slightly stronger correlations than ViT-Small, likely due to its hierarchical structure that more closely resembles traditional CNNs. Holdout Retraining shows moderate but significant positive correlations, and is attractive in practice given its large computational advantages vis-a-vis the other proxies. Overall, simple proxies

such as Confidence and Holdout Retraining remain predictive for VTs, enabling scalable memorization-based unlearning without expensive Feldman-score computations.

Table 1. Spearman Correlation Coefficients Between Memorization and Proxies

Proxy	CIFAR-10			CIFAR-100		
	ResNet-18	ViT-Small	Swin-Tiny	ResNet-50	ViT-Small	Swin-Tiny
Conf	-0.80	-0.79	-0.88	-0.91	-0.85	-0.90
MaxConf	-0.76	-0.77	-0.85	-0.87	-0.80	-0.86
Ent	-0.75	-0.78	-0.85	-0.80	-0.77	-0.82
BA	-0.71	-0.63	-0.79	-0.89	-0.69	-0.78
HR	+0.67	+0.45	+0.64	+0.62	+0.50	+0.52

## 4.2. Unlearning Algorithms Performance on Vision Transformers

For these experiments,  $D_f$  comprises 3,000 examples, divided into  $M = 3$  partitions of  $N = 1,000$  examples each, representing the lowest, medium and highest proxy values. We apply each algorithm unlearning in the order of low  $\rightarrow$  medium  $\rightarrow$  high memorization, using memorization-proxy values. All results are averaged over three runs and we also present 95% confidence intervals.

Given that pre-trained transformer models have lower memorization, we anticipated that  $\theta_r$  might already perform well on  $D_f$ . To establish a baseline for comparison, we calculated ToW and ToW-MIA parametrized by  $(\theta_o, \theta_r, D_f, D_r, D_{test})$  denoted as “Original”. This baseline indicates the performance we would achieve without applying any unlearning algorithm. Hyper-parameters for all algorithms are detailed in Appendix A.2.2.

### How do different MU approaches perform on VTs?

Figures 1 present unlearning results across both VTs and CIFAR-100 (see Figure 5 and 7 in Appendix for results on CIFAR-10 and SVHN). Our results show that simple approaches like Fine-tune perform surprisingly well, especially on the simpler SVHN dataset. NegGrad+ is consistently strong in all cases, and especially for more complex datasets (CIFAR-100) and outperforms all when paired with Holdout Retraining. Notably, NegGrad+ with Holdout Retraining for Swin-T shows even better performance than in ResNets. SalUn achieves good ToW scores but struggles with ToW-MIA on more complex datasets (CIFAR-100), though it performs competitively on SVHN. From the proxy viewpoint, Holdout Retraining performs excellently compared to Confidence for CIFAR-10/CIFAR-100, while Confidence can match it for the simpler SVHN. More detailed data can be found in Table 13.

**Key Takeaways.** SOTA MU algorithms from CNNs can be equally (if not more) effective for VTs. NegGrad+ is the most robust MU method for VTs, while SalUn is vulnerable in ToW-MIA on harder datasets. Proxy choice (Holdout Retraining vs. Confidence) further shapes outcomes.

**How does unlearning performance in VTs compare to CNNs?** We first compare the accuracy of the retrained model  $\theta_r$  on  $D_f$  in ResNets versus VTs, since this directly influences ToW and ToW-MIA evaluation for the benchmark model  $\theta_r$ . Table 2 shows that on CIFAR-10,  $\theta_r$  achieves much higher  $D_f$  accuracy in VTs than CNNs (e.g.,  $> 90\%$  for ViT/Swin-T vs.  $\sim 50\%$  for ResNet-18). This advantage stems from VT pretraining, which enables learning robust feature representations. Thus, after  $D_f$  examples are removed and the model is retrained,  $\theta_r$  remains close to the original  $\theta_o$  for VTs, explaining their high baseline “Original” performance (Table 13). However, this pretraining advantage diminishes on the more complex datasets (CIFAR-100).

Figure 1 (and Figure 5 in Appendix) shows how method rankings shift across architectures and proxies. With the Confidence proxy, Fine-tune and NegGrad+ perform best in ResNets, while VTs lag slightly. Under Holdout Retraining, however, VTs close or surpass this gap, particularly for NegGrad+. SalUn behaves differently: it achieves good ToW scores in VTs but underperforms on ToW-MIA compared to CNNs, suggesting that while it effectively adjusts transformer outputs to match  $\theta_r$ , it struggles to protect against MIAs.

**Key Takeaways.** Pretraining gives VTs an advantage on simpler tasks, but this weakens with increasing complexity. MU method rankings from CNNs do not transfer to VTs; they depend strongly on architectures and proxies. Holdout Retraining narrows or reverses the gap in favor of VTs.

Table 2.  $D_f$  accuracies of model  $\theta_r$  across architectures.

Architecture	CIFAR-10		CIFAR-100	
	Confidence	Holdout Retraining	Confidence	Holdout Retraining
ResNet-18	50.433 $\pm$ 6.808	62.922 $\pm$ 4.681	-	-
ResNet-50	-	-	64.267 $\pm$ 0.504	69.856 $\pm$ 2.620
ViT-Small	94.089 $\pm$ 0.456	89.244 $\pm$ 1.321	69.322 $\pm$ 1.788	68.767 $\pm$ 3.828
Swin-Tiny	91.867 $\pm$ 1.711	86.389 $\pm$ 1.246	69.833 $\pm$ 1.242	70.267 $\pm$ 2.848

### 4.3. How do VT architectures and capacities affect MU performance?

We observe systematic differences between ViT and Swin-T, as well as clear effects of model size.

**Architecture.** Swin-T exhibits stronger memorization than ViT (e.g., higher mean Feldman scores, heavier tails on CIFAR-10:  $\mu=0.17$  vs. 0.09, see Figures 3 and 4), which likely explains its superior performance with gradient-based methods such as NegGrad+. Swin-T also aligns with CNN-like behavior in SalUn, achieving optimal performance at saliency threshold  $\gamma = 0.3$ , consistent with CNNs (Zhao et al., 2024), whereas ViT requires a much lower  $\gamma = 0.1$ . This suggests that ViT’s global attention leads to more diffuse parameter involvement, while Swin-T’s local windowed attention allows for more concentrated, tar-

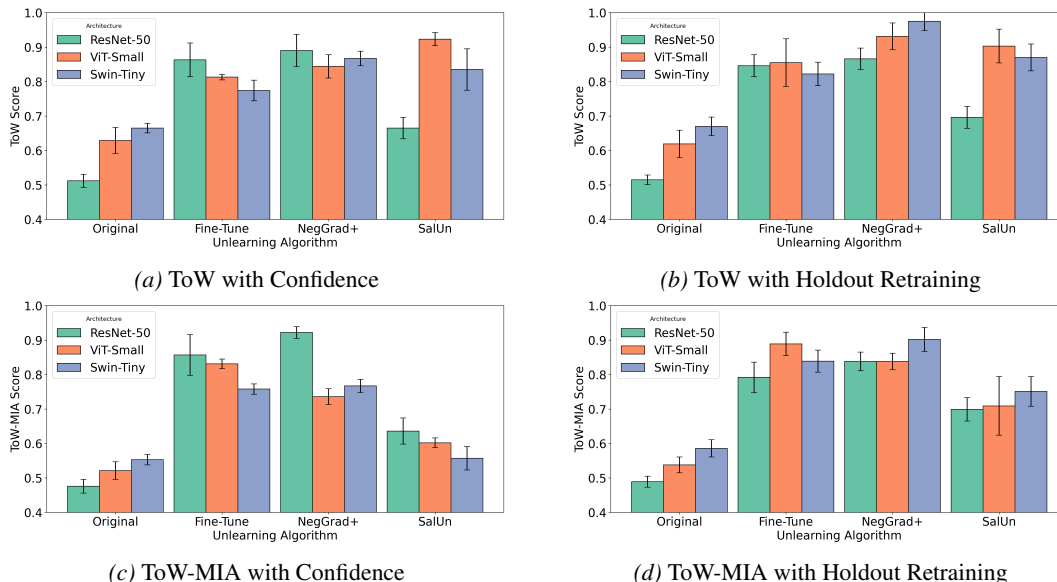


Figure 1. MU performance comparison on CIFAR-100.

geted unlearning. In terms of algorithm performance, Figure 1 (and Figure 5, Table 13 in Appendix) shows that Fine-tune is particularly effective on ViT (e.g., ToW-MIA=0.919 on CIFAR-10, 0.831 on CIFAR-100), while NegGrad+ excels on Swin-T, especially with Holdout Retraining on more complex tasks (e.g., ToW=0.975, ToW-MIA=0.902 on CIFAR-100). SalUn consistently attains good ToW but struggles on ToW-MIA, especially for ViT-Small (e.g., 0.582 on CIFAR-10 with Confidence). Dataset-level effects mirror these trends: ViT has an edge on the smaller, medium-complexity CIFAR-10, Swin-T dominates on the larger, more complex CIFAR-100, and both perform well on the simpler SVHN dataset. Continual unlearning results in Section 4.5 show broadly similar trends across ViT and Swin-T.

**Key Takeaways.** ViT favors fine-tuning-based unlearning, likely due to its global attention. Swin-T better supports gradient-based unlearning (NegGrad+) likely due to its local, hierarchical attention. Dataset complexity further shapes which family is most effective.

**Capacity.** To study the effect of model capacity, we extend our analysis to smaller and larger variants within each family, evaluated on CIFAR-10: ViT-Tiny ( $\sim 5.5$ M params) vs. ViT-Small ( $\sim 21.6$ M) and Swin-Tiny ( $\sim 27.5$ M) vs. Swin-Small ( $\sim 48.8$ M). We focus on the Holdout Retraining (HR) proxy, which was especially promising in earlier results. We report ToW and ToW-MIA for the three MU algorithms (Fine-tune, NegGrad+, SalUn) alongside the Original baseline in Table 3. The headline findings continue to hold: Fine-tune and NegGrad+ remain consistently strong; SalUn attains high ToW but is often much weaker on ToW-

MIA and is notably sensitive to model size, architecture, and proxy choice. We also observe *architecture-specific capacity trends*: For Swin-T, increasing capacity from Tiny to Small offers little ToW improvement and can reduce ToW-MIA, suggesting Swin-Tiny is already sufficient for CIFAR-10 and that Swin-Small may overfit. For ViT, the opposite holds: ViT-Tiny underperforms ViT-Small on both ToW and ToW-MIA, implying under-capacity limits MU effectiveness. The results reveal a “sweet spot” around ViT-Small and Swin-Tiny, where models are neither under- nor overfitting, yielding balanced unlearning-privacy.

Table 3. ToW and ToW-MIA on CIFAR-10 with HR across four VT architectures.

Algorithm	ViT-Small	ViT-Tiny	Swin-Small	Swin-Tiny
Original	$0.891 \pm 0.016$	$0.773 \pm 0.020$	$0.886 \pm 0.013$	$0.862 \pm 0.008$
Fine-tune	$0.928 \pm 0.013$	$0.862 \pm 0.060$	$0.921 \pm 0.005$	$0.923 \pm 0.021$
NegGrad+	$0.916 \pm 0.016$	$0.957 \pm 0.011$	$0.944 \pm 0.028$	$0.977 \pm 0.023$
SalUn	$0.956 \pm 0.003$	$0.846 \pm 0.043$	$0.950 \pm 0.031$	$0.961 \pm 0.048$

(a) ToW

Algorithm	ViT-Small	ViT-Tiny	Swin-Small	Swin-Tiny
Original	$0.831 \pm 0.014$	$0.699 \pm 0.020$	$0.832 \pm 0.020$	$0.811 \pm 0.018$
Fine-tune	$0.913 \pm 0.008$	$0.854 \pm 0.060$	$0.924 \pm 0.010$	$0.931 \pm 0.021$
NegGrad+	$0.968 \pm 0.015$	$0.869 \pm 0.011$	$0.888 \pm 0.021$	$0.924 \pm 0.028$
SalUn	$0.766 \pm 0.039$	$0.640 \pm 0.043$	$0.568 \pm 0.093$	$0.834 \pm 0.022$

(b) ToW-MIA

**Key Takeaways.** Performance trends remain stable across ViT-Tiny/Small and Swin-Tiny/Small.

#### 4.4. Results on Larger/More Complex Data

To examine unlearning larger-scale, more complex conditions, we leverage that our Vision Transformers are pretrained on ImageNet-1K and use the *validation* split (50,000 images unseen during pretraining) as a new evaluation dataset (already  $5\times$  larger than CIFAR-100’s test set). We form a forget set of  $|D_f|=3,000$  (partitioned into three 1k subsets for low/medium/high proxy values, as in Section 4.2), and treat the remaining 47k images as retain/test set. As this setup has only retain/test and forget components, we report ToW and ToW-MIA with two terms (retain/test accuracy and forget accuracy). We evaluate on the (more appropriate) larger Swin-Small (48.8M params) and use the Holdout Retraining proxy since it was previously found to be high performing.

Table 4. Unlearning performance with HR proxy for Swin-Small on the 50k ImageNet-1K validation set.

Algorithm	ToW	ToW-MIA
Fine-tune	$0.780 \pm 0.023$	$0.747 \pm 0.009$
NegGrad+	$0.819 \pm 0.018$	$0.772 \pm 0.034$
SalUn	$0.743 \pm 0.027$	$0.647 \pm 0.030$

Table 4 shows that the key earlier conclusions continue to hold at this larger scale: *NegGrad+* and *Fine-tune* perform strongly, while *SalUn* again underperforms, especially on ToW-MIA. This reinforces the conclusion that comparatively simple unlearning strategies can be effective even for larger models and datasets, albeit performance varies with architecture and data complexity. We also note that absolute ToW/ToW-MIA values are lower here than for Swin-Tiny on CIFAR-100, despite Swin-Small’s larger capacity. This is reasonable: (i) retain/test accuracy is harder given ImageNet’s larger scale, diversity, and label space, and (ii) forgetting is more challenging on richer ImageNet images (greater embedding entanglement). Consequently, both terms in ToW and ToW-MIA are pressured downward relative to the CIFAR-100 setting, and further gains would likely require even larger-capacity models and/or stronger regularization. Finally, Table 5 reinforces our earlier observation that the benefit of pretraining for forget accuracy diminishes as task complexity increases (compared to Table 2).

**Key Takeaways.** Simple methods (NegGrad+, Fine-tune)

Table 5.  $D_f$  accuracies of Retrained  $\theta_r$  (with HR) across architectures on the 50k ImageNet-1K validation set.

Architecture	$D_f$ accuracy (%)
ResNet-50	$69.139 \pm 1.722$
Swin-Small	$69.433 \pm 2.246$

remain effective even on ImageNet-scale data, whereas SalUn underperforms, and the benefits of pretraining diminish as complexity grows.

**Model scaling on ImageNet-1K.** To further examine capacity effects under ImageNet-scale complexity, we additionally evaluate larger VT variants, Swin-Base ( $\sim 88$ M parameters) and ViT-Base/16 ( $\sim 85$ M parameters), under the same ImageNet-1K validation protocol and HR proxy.

Table 6 shows that increasing model capacity leads to modest but consistent performance gains within the Swin family. Importantly, the qualitative trends observed for smaller models persist across all architectures at this scale: Fine-tune and NegGrad+ remain strong performers, whereas SalUn continues to underperform.

Table 6. Unlearning performance on ImageNet-1K validation set with HR proxy, comparing model scaling within the Swin family, as well as results for ViT-Base/16.

Method	Swin-Small (49M)	Swin-Base (88M)	ViT-Base/16 (85M)
Fine-tune	$0.780 \pm 0.023$	$0.808 \pm 0.007$	$0.843 \pm 0.016$
NegGrad+	$0.819 \pm 0.018$	$0.837 \pm 0.004$	$0.842 \pm 0.005$
SalUn	$0.743 \pm 0.027$	$0.746 \pm 0.013$	$0.773 \pm 0.027$

**Key Takeaways.** Increasing model capacity at ImageNet scale yields small but consistent improvements, and method-level trends remain consistent.

#### 4.5. Does Continual Unlearning Impact Performance in Vision Transformers?

In practical deployments, unlearning is often performed continually, through a sequence of smaller forget operations rather than a single large one. We therefore examine whether repeated unlearning leads to cumulative degradation in performance. Based on earlier results, we focus on NegGrad+ with Holdout Retraining, which is the best-performing algorithm-proxy pair. We perform five sequential unlearning steps, unlearning the same total number of examples ( $|D_f| = 3,000$ ). At each step, proxy values are recomputed, and the forget set is partitioned as before, with  $|D_f| = 600$  per step and  $N = 200$  examples per partition.

Figure 2 shows unlearning performance across the five steps on CIFAR-100. We observe stable behavior across metrics and architectures. While ViT-Small exhibits a mild downward trend, all metrics remain within the confidence intervals of the initial unlearning step and are comparable to single-step results reported in Section 4.2. Similar trends hold for CIFAR-10 and SVHN (Table 16, Appendix A.5.2 for CIFAR-10 and A.8.2 for SVHN).

To further stress-test continual unlearning, we extend this evaluation to ten sequential unlearning steps under the same setting (NegGrad+ with HR), using both ViT-Small and Swin-Tiny. As shown in Table 17, performance re-

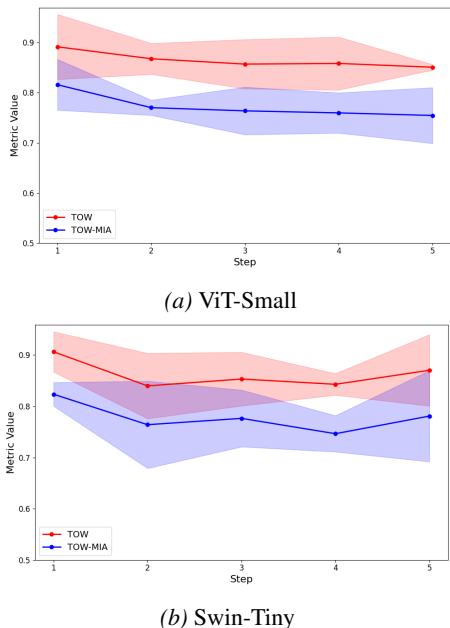


Figure 2. Continual Unlearning Performance Across Five Steps on CIFAR-100, reported with 95% confidence intervals.

mains stable across steps, with no evidence of substantial accumulated degradation in either ToW or ToW-MIA. These results reinforce the earlier observation that suitable method-proxy pairs can support continual unlearning without progressive performance degradation.

**Key Takeaway.** Minimal (if any) degradation occurs under continual unlearning in VTs.

### 5. Practitioners Takeaways

Our results yield several actionable guidelines for applying machine unlearning in VTs.

**Architecture–method compatibility is critical:** ViT models consistently favor Fine-tune, likely due to their global attention and diffuse parameter involvement, while Swin architectures pair best with NegGrad+, which benefits from local and hierarchical inductive biases. SalUn, although competitive in ToW, is unreliable in ToW-MIA for VTs (especially ViT) and should be avoided in privacy-sensitive settings.

**Memorization proxy choice further shapes performance.** Confidence is the highest-fidelity proxy overall and works well on simpler datasets, whereas Holdout Retraining (HR) yields the strongest and most stable unlearning performance on complex datasets and under continual unlearning. In practice:

- ViT + Fine-tune + Confidence is effective and efficient for low-to-moderate memorization regimes.

- Swin + NegGrad+ + HR is the most robust choice for high-complexity or continual unlearning scenarios.
- Stable unlearning is achieved using small learning rates, cosine scheduling, and sequential partitioning from low → high memorization.

### 6. Conclusions

We benchmarked the performance of fundamentally different approaches to MU, ranging from simpler baselines to more advanced SOTA unlearning algorithms in VTs. We focused on algorithms leveraging memorization, as memorization has been found to be key to unlearning (across modalities) and the SOTA MU approaches for vision tasks can be substantially improved by leveraging it. To ensure the practicality of leveraging memorization, we studied memorization patterns in VTs and five different memorization proxies that have been found to offer high memorization-score fidelity in CNNs while being drastically more efficient to compute. We employed different datasets to account for the effects of varying sizes and complexities. We studied two different popular VT architectures (ViT and Swin-T) selected to be closer or further from CNN inductive biases. We also used different model capacities to see the impact of capacities on MU performance (with carefully selected dataset sizes to avoid over- and under-fitting). This work represents the first comprehensive study in this domain and sheds new light on the current state of affairs of MU algorithm performance in VTs.

This work contributes the following novel insights: (i) Pre-training of VTs can help improve unlearning for smaller and simpler datasets/tasks. (ii) VTs and CNNs largely exhibit the same memorization patterns. (iii) Well-known memorization proxies from CNNs can benefit unlearning performance in VTs as they can do in CNNs. (iv) Continual unlearning does not degrade the efficacy of memorization proxies and overall unlearning performance in VTs. (v) VTs can enjoy similar, if not better, unlearning performance to that in CNNs (using CNN-derived algorithms). (vi) Swin-T can outperform ViT on more complex datasets, due to Swin-T’s architectural similarities to CNNs. (vii) NegGrad+, perhaps surprisingly, emerges as a consistent, strong performer for VTs, especially on more complex datasets. (viii) Holdout Retraining emerges as the proxy yielding superior unlearning performance in VTs, whereas Confidence can be competitive on lower-complexity datasets. We hope these insights, as well as the associated publicly available codebase/dataset infrastructure benchmark, will springboard the study of MU in VTs, serving as a basis upon which to add new (future) algorithms, especially developed for VTs.

## References

- George-Octavian Barbulescu and Peter Triantafillou. To each (textual sequence) its own: Improving memorized-data unlearning in large language models. In *International Conference on Machine Learning (ICML)*, 2024. URL <https://arxiv.org/abs/2405.03097>.
- Xavier F. Cadet, Anastasia Borovykh, Mohammad Malekzadeh, Sara Ahmadi-Abhari, and Hamed Haddadi. Deep unlearn: Benchmarking machine unlearning, 2024. URL <https://arxiv.org/abs/2410.01276>.
- Yinzhi Cao and Junfeng Yang. Towards making systems forget with machine unlearning. In *2015 IEEE Symposium on Security and Privacy*, pages 463–480, 2015. doi: 10.1109/SP.2015.35.
- Nicholas Carlini, Úlfar Erlingsson, and Nicolas Papernot. Distribution density, tails, and outliers in machine learning: Metrics and applications, 2019. URL <https://arxiv.org/abs/1910.13427>.
- Jiali Cheng and Hadi Amiri. Mu-bench: A multitask multimodal benchmark for machine unlearning, 2024. URL <https://arxiv.org/abs/2406.14796>.
- Ikhyn Cho, Changyeon Park, and Julia Hockenmaier. Vitmul: A baseline study on recent machine unlearning methods applied to vision transformers, 2024. URL <https://arxiv.org/abs/2403.09681>.
- Jia Deng, Wei Dong, Richard Socher, Li-Jia Li, Kai Li, and Li Fei-Fei. Imagenet: A large-scale hierarchical image database. In *2009 IEEE Conference on Computer Vision and Pattern Recognition*, pages 248–255. IEEE, 2009. doi: 10.1109/CVPR.2009.5206848.
- Alexey Dosovitskiy, Lucas Beyer, Alexander Kolesnikov, Dirk Weissenborn, Xiaohua Zhai, Thomas Unterthiner, Mostafa Dehghani, Matthias Minderer, Georg Heigold, Sylvain Gelly, Jakob Uszkoreit, and Neil Houlsby. An image is worth 16x16 words: Transformers for image recognition at scale, 2021. URL <https://arxiv.org/abs/2010.11929>.
- Chongyu Fan, Jiancheng Liu, Yihua Zhang, Eric Wong, Dennis Wei, and Sijia Liu. Salun: Empowering machine unlearning via gradient-based weight saliency in both image classification and generation, 2024. URL <https://arxiv.org/abs/2310.12508>.
- Vitaly Feldman. Does learning require memorization? a short tale about a long tail, 2019. URL <https://arxiv.org/abs/1906.05271>.
- Vitaly Feldman and Chiyuan Zhang. What neural networks memorize and why: Discovering the long tail via influence estimation, 2020. URL <https://pluskid.github.io/influence-memorization/>.
- Antonio Ginart, Melody Y. Guan, Gregory Valiant, and James Zou. Making ai forget you: Data deletion in machine learning, 2019. URL <https://arxiv.org/abs/1907.05012>.
- Shashwat Goel, Ameya Prabhu, and Ponnurangam Kumaraguru. Evaluating inexact unlearning requires revisiting forgetting, 01 2022.
- Aditya Golatkar, Alessandro Achille, and Stefano Soatto. Eternal sunshine of the spotless net: Selective forgetting in deep networks, 2020. URL <https://arxiv.org/abs/1911.04933>.
- Keltin Grimes, Collin Abidi, Cole Frank, and Shannon Gallagher. Gone but not forgotten: Improved benchmarks for machine unlearning, 2024. URL <https://arxiv.org/abs/2405.19211>.
- Joel Jang, Dongkeun Yoon, Sohee Yang, Sungmin Cha, Moontae Lee, Lajanugen Logeswaran, and Minjoon Seo. Knowledge unlearning for mitigating privacy risks in language models, 2022. URL <https://arxiv.org/abs/2210.01504>.
- Jinghan Jia, Jiancheng Liu, Parikshit Ram, Yuguang Yao, Gaowen Liu, Yang Liu, Pranay Sharma, and Sijia Liu. Model sparsity can simplify machine unlearning. *Advances in Neural Information Processing Systems*, 36:51584–51605, 2023. URL [https://proceedings.neurips.cc/paper\\_files/paper/2023/file/a204aa68ab4e970e1ceccfb5b5cdc5e4-Paper-Conference.pdf](https://proceedings.neurips.cc/paper_files/paper/2023/file/a204aa68ab4e970e1ceccfb5b5cdc5e4-Paper-Conference.pdf).
- Jinghan Jia, Jiancheng Liu, Parikshit Ram, Yuguang Yao, Gaowen Liu, Yang Liu, Pranay Sharma, and Sijia Liu. Model sparsity can simplify machine unlearning, 2024. URL <https://arxiv.org/abs/2304.04934>.
- Ziheng Jiang, Chiyuan Zhang, Kunal Talwar, and Michael C. Mozer. Characterizing structural regularities of labeled data in overparameterized models, 2021. URL <https://arxiv.org/abs/2002.03206>.
- Alex Krizhevsky. Learning multiple layers of features from tiny images. *University of Toronto*, 2009. URL <https://www.cs.toronto.edu/~kriz/learning-features-2009-TR.pdf>.
- Meghdad Kurmanji, Peter Triantafillou, Jamie Hayes, and Eleni Triantafillou. Towards unbounded machine unlearning. In *2023 Thirty-Seventh Annual Conference*

- on *Neural Information Processing Systems (NeurIPS)*, 2023. URL <https://arxiv.org/abs/2302.09880>.
- Nathaniel Li, Alexander Pan, Anjali Gopal, Summer Yue, Daniel Berrios, Alice Gatti, Justin D. Li, Ann-Kathrin Dombrowski, Shashwat Goel, Long Phan, Gabriel Mukobi, Nathan Helm-Burger, Rassin Lababidi, Lennart Justen, Andrew B. Liu, Michael Chen, Isabelle Barrass, Oliver Zhang, Xiaoyuan Zhu, Rishub Tamirisa, Bhrgu Bharathi, Adam Khoja, Zhenqi Zhao, Ariel Herbert-Voss, Cort B. Breuer, Samuel Marks, Oam Patel, Andy Zou, Mantas Mazeika, Zifan Wang, Palash Oswal, Weiran Lin, Adam A. Hunt, Justin Tienken-Harder, Kevin Y. Shih, Kemper Talley, John Guan, Russell Kaplan, Ian Steneker, David Campbell, Brad Jokubaitis, Alex Levinson, Jean Wang, William Qian, Kallol Krishna Karmakar, Steven Basart, Stephen Fitz, Mindy Levine, Ponnurangam Kumaraguru, Uday Tupakula, Vijay Varadharajan, Ruoyu Wang, Yan Shoshitaishvili, Jimmy Ba, Kevin M. Esvelt, Alexandr Wang, and Dan Hendrycks. The wmdp benchmark: Measuring and reducing malicious use with unlearning, 2024. URL <https://arxiv.org/abs/2403.03218>.
- Ze Liu, Yutong Lin, Yue Cao, Han Hu, Yixuan Wei, Zheng Zhang, Stephen Lin, and Baining Guo. Swin transformer: Hierarchical vision transformer using shifted windows, 2021. URL <https://arxiv.org/abs/2103.14030>.
- Rui Ma, Qiang Zhou, Yizhu Jin, Daquan Zhou, Bangjun Xiao, Xiuyu Li, Yi Qu, Aishani Singh, Kurt Keutzer, Jingtong Hu, Xiaodong Xie, Zhen Dong, Shanghang Zhang, and Shiji Zhou. A dataset and benchmark for copyright infringement unlearning from text-to-image diffusion models, 2024. URL <https://arxiv.org/abs/2403.12052>.
- Pratyush Maini, Zhili Feng, Avi Schwarzschild, Zachary C. Lipton, and J. Zico Kolter. Tofu: A task of fictitious unlearning for llms, 2024. URL <https://arxiv.org/abs/2401.06121>.
- Seth Neel, Aaron Roth, and Saeed Sharifi-Malvajerdi. Descent-to-delete: Gradient-based methods for machine unlearning, 2020. URL <https://arxiv.org/abs/2007.02923>.
- Yuval Netzer, Tao Wang, Adam Coates, Alessandro Bisacco, Bo Wu, and Andrew Y. N. Reading digits in natural images with unsupervised feature learning. In *NIPS Workshop on Deep Learning and Unsupervised Feature Learning*, 2011.
- Jie Ren, Yaxin Li, Shenglai Zeng, Han Xu, Lingjuan Lyu, Yue Xing, and Jiliang Tang. Unveiling and mitigating memorization in text-to-image diffusion models through cross attention, 2024. URL <https://arxiv.org/abs/2403.11052>.
- Ayush Sekhari, Jayadev Acharya, Gautam Kamath, and Ananda Theertha Suresh. Remember what you want to forget: Algorithms for machine unlearning, 2021. URL <https://arxiv.org/abs/2103.03279>.
- Anvith Thudi, Gabriel Deza, Varun Chandrasekaran, and Nicolas Papernot. Unrolling sgd: Understanding factors influencing machine unlearning, 2022. URL <https://arxiv.org/abs/2109.13398>.
- Reihaneh Torkzadehmahani, Reza Nasirigerdeh, Georgios Kaissis, Daniel Rueckert, Gintare Karolina Dziugaite, and Eleni Triantafillou. Improved localized machine unlearning through the lens of memorization. *arXiv preprint arXiv:2412.02432*, 2024.
- Eleni Triantafillou, Peter Kairouz, Fabian Pedregosa, Jamie Hayes, Meghdad Kurmanji, Kairan Zhao, Vincent Dumoulin, Julio Jacques Junior, Ioannis Mitliagkas, Jun Wan, Lisheng Sun Hosoya, Sergio Escalera, Gintare Karolina Dziugaite, Peter Triantafillou, and Isabelle Guyon. Are we making progress in unlearning? findings from the first neurips unlearning competition, 2024. URL <https://arxiv.org/abs/2406.09073>.
- Ashish Vaswani, Noam Shazeer, Niki Parmar, Jakob Uszkoreit, Llion Jones, Aidan N. Gomez, Lukasz Kaiser, and Illia Polosukhin. Attention is all you need. *CoRR*, abs/1706.03762, 2017. URL <http://arxiv.org/abs/1706.03762>.
- Alexander Warnecke, Lukas Pirch, Christian Wressnegger, and Konrad Rieck. Machine unlearning of features and labels, 2023. URL <https://arxiv.org/abs/2108.11577>.
- Yuxin Wen, Yuchen Liu, Chen Chen, and Lingjuan Lyu. Detecting, explaining, and mitigating memorization in diffusion models, 2024. URL <https://arxiv.org/abs/2407.21720>.
- Ross Wightman. Pytorch image models. <https://github.com/huggingface/pytorch-image-models>, 2019.
- Heng Xu, Tianqing Zhu, Lefeng Zhang, Wanlei Zhou, and Philip S. Yu. Machine unlearning: A survey, 2023. URL <https://arxiv.org/abs/2306.03558>.
- Yihua Zhang, Chongyu Fan, Yimeng Zhang, Yuguang Yao, Jinghan Jia, Jiancheng Liu, Gaoyuan Zhang, Gaowen Liu, Ramana Rao Kompella, Xiaoming Liu, and Sijia

Liu. Unlearncanvas: Stylized image dataset for enhanced machine unlearning evaluation in diffusion models, 2024. URL <https://arxiv.org/abs/2402.11846>.

Kairan Zhao, Meghdad Kurmanji, George-Octavian Bărbulescu, Eleni Triantafillou, and Peter Triantafillou. What makes unlearning hard and what to do about it. *Advances in Neural Information Processing Systems*, 37: 12293–12333, 2024.

## A. Appendix

### A.1. Impact Statement & Limitations

**Impact Statement.** This work advances privacy-preserving Vision Transformers by examining how architectural design choices affect the effectiveness of machine unlearning. Through a systematic evaluation across model architectures, scales, and data complexity, we identify key factors that influence reliable data removal. These findings provide practical guidance for developing vision models that better support “right to be forgotten” requirements, contributing to more trustworthy deployment in sensitive real-world settings.

**Limitations.** Our benchmarking setup represents a practical compromise in terms of VT models, their sizes, and the size and complexity of datasets, allowing for insightful comparisons to CNNs, while studying fundamental approaches to MU. Nonetheless, there is much more work to follow, adding more datasets, more models and capacities, more (new and existing) algorithms, and different metrics.

### A.2. Implementation Details

This section outlines the key implementation details for all experiments conducted in this study. For all experiments involving transformer architectures, we fine-tune models initialized with ImageNet-1k pretrained weights provided by the `timm` library (Wightman, 2019), as described in Section 3.2.

All experiments on the CIFAR-10 and CIFAR-100 datasets were conducted using a mix of NVIDIA RTX 2080 Ti, NVIDIA A10 and NVIDIA TITAN Xp GPUs, taking roughly 210 GPU hours. For the experiments on the SVHN dataset, training and evaluation were performed on NVIDIA A5000 GPUs, which consumed approximately 300 GPU hours.

The code for reproducing the results is available at: [https://github.com/kairanzhao/Unlearning\\_VTs](https://github.com/kairanzhao/Unlearning_VTs)

#### A.2.1. MEMORIZATION ESTIMATION

For memorization estimation, we use ResNet-18 for CIFAR-10 and rely on precomputed memorization scores provided by (Feldman and Zhang, 2020) for CIFAR-100. Additionally, we compute memorization scores using ViT-Small and Swin-Tiny architectures for both CIFAR-10 and CIFAR-100. The training configurations and corresponding hyperparameters are summarized in Table 7.

Table 7. Training configurations along with hyper-parameters of the models used to compute memorization scores shown in Figures 3 and 4. The “Transformers” column represents the configuration for both ViT-Small and Swin-Tiny across CIFAR-10 and CIFAR-100.

	ResNet-18	Transformers
<b>Optimizer</b>	SGD	AdamW
<b>Base learning rate</b>	0.01	0.0001
<b>Loss</b>	Cross-Entropy	Cross-Entropy
<b>Learning rate scheduler</b>	Step decay	CosineAnnealingLR
<b>Batch size</b>	512	128
<b>Epochs</b>	30	30
<b>Momentum</b>	0.9	-
<b>Weight decay</b>	0.0005	0.05
<b>Data augmentation</b>	None	None

A.2.2. UNLEARNING

This section presents the configuration and hyper-parameter details used to obtain the necessary models for ToW and ToW-MIA: “Original”  $\theta_o$ , “Retrained”  $\theta_r$  and “Unlearned”  $\theta_u$ . Table 8 shows the hyper-parameter details for training original models & retraining. Table 9 shows the unlearning hyper-parameters, and Table 10 presents the sequential unlearning hyper-parameters.

Table 8. Training configurations and hyperparameter used for the original models ( $\theta_o$ ) and the retrained models ( $\theta_r$ ) on the CIFAR-10 and CIFAR-100 datasets.

Hyperparameter	ViT-Small & Swin-Tiny
<b>Optimizer</b>	AdamW
<b>Base learning rate</b>	0.0001
<b>Loss</b>	Cross-Entropy
<b>Learning rate scheduler</b>	CosineAnnealingLR
<b>Batch size</b>	128
<b>Epochs</b>	50
<b>Weight decay</b>	0.05
<b>Data augmentation</b>	Random Crop + Horizontal Flip

Table 9. Hyper-parameters across all unlearn methods within the RUM<sub>F</sub> meta-algorithm on both Confidence and Holdout Retraining proxies to derive the unlearn models  $\theta_u$ . “Unlearn Epochs” column refers to the performed number of epochs each algorithm performed for the three memorization partitions (low → medium → high) respectively.

Algorithm	Architecture	Unlearn Epochs	Unlearn LR	$\beta$	$\alpha$	$\gamma$
FineTune	ViT-Small	5,5,10	0.0001	-	-	-
	Swin-Tiny	5,5,10	0.0001	-	-	-
NegGrad+	ViT-Small	5,5,10	0.00002	0.97	-	-
	Swin-Tiny	5,5,10	0.00002	0.97	-	-
SalUn	ViT-Small	5,5,10	0.00005	-	1	0.1
	Swin-Tiny	5,5,10	0.0002	-	1	0.3

Table 10. Hyper-parameters at each sequential unlearning step for the NegGrad+ and Holdout Retraining configuration utilized. “Unlearn Epochs” are reduced to 1 for partition (low → medium → high) due to the smaller forget set size ( $|D_f| = 600$ ) at each step. All other settings remain consistent with the primary experiments.

Unlearn Epochs	Unlearn LR	$\beta$
1,1,1	0.00002	0.97

A.3. Memorization and Proxies in VTs

A.3.1. DO VISION TRANSFORMERS MEMORIZE THE SAME WAY AS CNNs?

As memorization plays a key role in unlearning, this step is critical. For ResNet-18/CIFAR-10 and both VTs for both datasets, the training configuration is detailed in Table 7 (Appendix A.2.1). For ResNet-50/CIFAR-100, scores were already pre-computed (Feldman and Zhang, 2020).

Figures 3 (and 4) present the memorization distributions across different architectures for CIFAR-100 (CIFAR-10). In all cases we see similarly skewed distributions, consistent with the “long-tail” discovery in (Feldman and Zhang, 2020). For CIFAR-100, in particular, both VTs closely align with ResNet-50. Hence, despite architectural differences between VTs and CNNs, their memorization patterns remain fundamentally similar, especially for more complex tasks. This provides a foundation for studying unlearning a la RUM in VTs.

For CIFAR-100, we observe that both VTs closely align with ResNet-50 in terms of memorization. However, on CIFAR-10, VTs exhibit slightly lower memorization compared to ResNet-18. This can be attributed to the fact that pre-trained VTs benefit from a stronger ability to capture global contextual information, which reduces their reliance on memorizing training examples when adapting to simpler tasks. This advantage, however, does not extend to more challenging tasks like CIFAR-100.

A.3.2. ARE CNN-DERIVED MEMORIZATION PROXIES RELEVANT FOR VTs?

Differences in architecture (e.g., inductive biases) and in training (e.g., finetune-then-retrain in VTs) raise doubts about the appropriateness of CNN memorization proxies for VTs.

We first provide the formulas for computing each of the following proxies: Confidence (C), Max Confidence (MaxC), Entropy (E), Binary Accuracy (BA) (Jiang et al., 2021) and Holdout Retraining (HR) (Carlini et al., 2019).

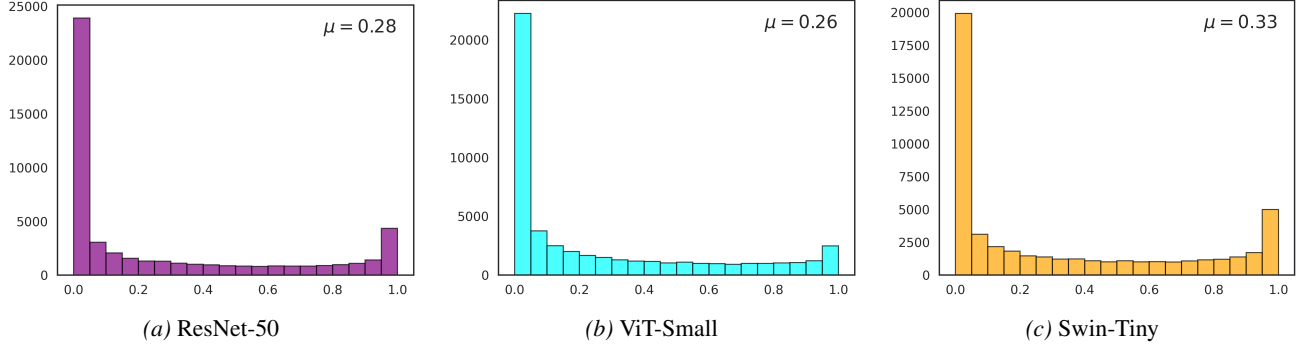


Figure 3. Memorization histograms across different architectures on CIFAR-100

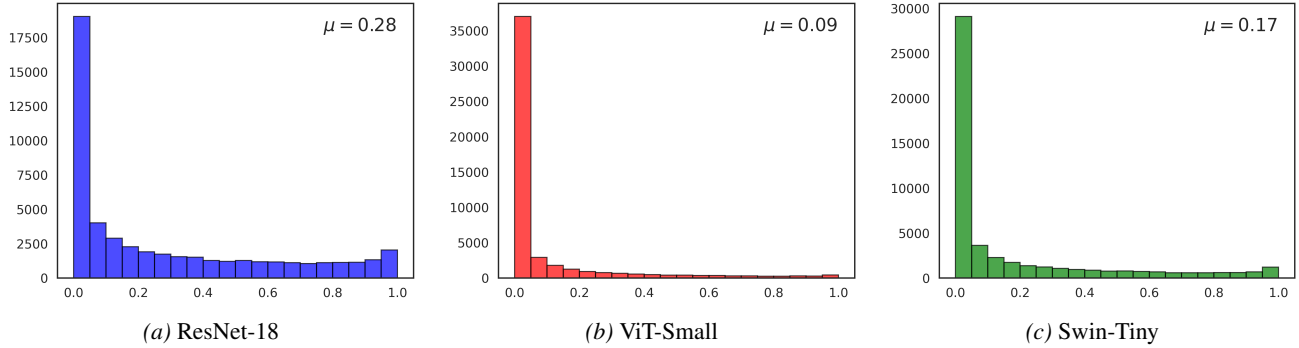


Figure 4. Memorization histograms across different architectures on CIFAR-10

$$\text{Conf}(x_i, y_i) = \frac{1}{E} \sum_{e=1}^E P_{\theta_e}(y = y_i | x_i), \quad (4a)$$

$$\text{MaxConf}(x_i) = \frac{1}{E} \sum_{e=1}^E \max_y P_{\theta_e}(y | x_i), \quad (4b)$$

$$\text{Ent}(x_i) = \frac{1}{E} \sum_{e=1}^E \sum_y P_{\theta_e}(y | x_i) \log P_{\theta_e}(y | x_i), \quad (4c)$$

$$\text{BA}(x_i, y_i) = \frac{1}{E} \sum_{e=1}^E \mathbb{1} \left[ \arg \max_y P_{\theta_e}(y | x_i) = y_i \right], \quad (4d)$$

$$\text{HR}(x_i) = \text{symKL}(p_{\theta_o}(x_i) \| p_{\theta'}(x_i)). \quad (4e)$$

Results in Table 1 answer the question in the affirmative. Proxies were calculated using models trained with identical hyper-parameters as those used to derive memorization scores (see Table 7 in Appendix A.2.1).

Confidence consistently demonstrates the strongest correlation across all models and datasets. The correlation magnitude for VTs largely resembles that of CNNs – further evidence that memorizations are fundamentally similar across these architectures. Swin-Tiny generally has stronger cor-

Table 11. Spearman correlation coefficients between memorization and proxies (duplicate of Table 1, included here for completeness)

Proxy	CIFAR-10			CIFAR-100		
	ResNet-18	ViT-Small	Swin-Tiny	ResNet-50	ViT-Small	Swin-Tiny
Conf	-0.80	-0.79	-0.88	-0.91	-0.85	-0.90
MaxConf	-0.76	-0.77	-0.85	-0.87	-0.80	-0.86
Ent	-0.75	-0.78	-0.85	-0.80	-0.77	-0.82
BA	-0.71	-0.63	-0.79	-0.89	-0.69	-0.78
HR	+0.67	+0.45	+0.64	+0.62	+0.50	+0.52

relations compared to ViT-Small, possibly due to its hierarchical structure that more closely resembles traditional CNNs. Holdout Retraining shows more moderate positive (albeit still significant) correlations.

Based on these findings, we selected Confidence as the best-performing learning event proxy with consistently high absolute correlation values and Holdout Retraining as a representative of a different proxy category. Importantly, Holdout Retraining offers large computational advantages as it does not require monitoring model behaviour during training.

#### A.4. Ablation on Vanilla vs. RUM-Integrated Unlearning

To isolate the effect of the RUM framework, we conduct an additional ablation comparing vanilla unlearning algo-

gorithms against their RUM-integrated counterparts. Specifically, we evaluate Fine-tuning, NegGrad+, and SalUn, both with and without RUM. Experiments are performed on CIFAR-100 using ViT-Small and Swin-Tiny architectures.

The comparison in Table 12 provides a controlled reference point for assessing the benefit of incorporating unlearning algorithms into the RUM framework. Across all methods and architectures, the RUM-based variants consistently outperform their vanilla counterparts in both ToW and ToW-MIA, indicating more effective forgetting with improved resistance to membership inference.

These results complement prior findings reported for CNN-based models and further validate the generality of RUM across transformer architectures. Based on this evidence, we adopt the RUM-integrated versions of these algorithms throughout the main experimental evaluation.

### A.5. Results for CIFAR-10

This section presents the corresponding figures for the CIFAR-10 dataset that mirror the ones of CIFAR-100 found in Section 4.

#### A.5.1. UNLEARNING PERFORMANCE FOR CIFAR-10

**Algorithm-Level Comparison on CIFAR-10.** Figure 5 shows the unlearning performance results for the CIFAR-10 dataset. First, note that the original VT model (no unlearning) already achieves relatively high scores on CIFAR-10, which is unlike the results in CIFAR-100. This is consistent with our earlier observation that VTs exhibit lower memorization on this simpler dataset, reducing performance differences between  $\theta_o$  and  $\theta_r$  on  $D_f$ . Nevertheless, we see marginal improvements from unlearning algorithms on CIFAR-10, still making a case for their utilization in low-memorized data.

Taking a closer look, all methods in VTs appear to show smaller improvements in ToW compared to the original model. Additionally, there is no clear winner for VTs between the two proxy strategies. Again, these results are in contrast to the more substantial improvements observed on the more complex CIFAR-100 dataset. For instance, even a simple approach like Fine-tune significantly outperforms the original model across all configurations on CIFAR-100—an effect not observed here. More advanced algorithms show greater gains in ToW performance on CIFAR-100 than they do on CIFAR-10, compared to the original VT model.

**Architecture-Level Comparison on CIFAR-10.** Figure 5 also presents the architecture-wise comparison on CIFAR-10, analogous to the analysis shown for CIFAR-100 in Figure 1. We observe that VTs generally achieve higher ToW scores than ResNet-18, with NegGrad+ and

SalUn performing particularly well on both VTs. However, this performance gap is less evident in the ToW-MIA metrics, where Fine-tune shows comparable performance across all architectures. Notably, NegGrad+ is the only unlearning method that improves ToW-MIA for both proxies. In contrast, SalUn continues to struggle on ToW-MIA within VTs: ResNet-18 significantly outperforms VTs when using the Confidence proxy and matches their performance under Holdout Retraining.

#### A.5.2. CONTINUAL UNLEARNING FOR CIFAR-10

Figure 6 and Table 16 show the results in the same fashion as seen in Figure 2 for CIFAR-100. Here we observe an even higher stability in results with even more negligible degradation, further accentuated by the smaller performance gap between ToW and ToW-MIA than those seen for CIFAR-100. This, along with higher average scores, comes as no surprise due to the higher “Original” baseline performance exhibited by the VTs on CIFAR-10.

### A.6. Detailed ToW and ToW-MIA Results on CIFAR-10 and CIFAR-100

This section presents detailed ToW and ToW-MIA performance results for all evaluated architectures on the CIFAR-10 and CIFAR-100 datasets. These results for ViT-Small, Swin-Tiny (Table 13), and ResNets (Table 14) are used to generate Figures 1 and 5.

#### A.6.1. RESULTS FOR ViT-SMALL AND SWIN-TINY ACROSS ALL ALGORITHMS

Table 13 provides detailed ToW and ToW-MIA results for ViT-Small and Swin-Tiny on CIFAR-10/CIFAR-100. These values are used in the corresponding architecture and method comparison figures.

#### A.6.2. RESULTS FOR RESNET-18 AND RESNET-50 ACROSS ALL ALGORITHMS

Table 14 reports the detailed results for ResNet-18 (CIFAR-10) and ResNet-50 (CIFAR-100). These metrics support the comparative analysis shown in Figures 1 and 5. Further breakdowns of ToW and ToW-MIA (by individual terms) for Vision Transformer architectures across datasets are reported in Table 15.

### A.7. Continual Unlearning Results in VTs for CIFAR-10, CIFAR-100

Table 16 and Table 17 presents detailed ToW and ToW-MIA results of VTs architectures over CIFAR-10 and CIFAR-100, for five steps and ten steps, respectively. At each sequential unlearning step, we use the strong-performing combination of the NegGrad+ algorithm with

## Benchmarking Unlearning for Vision Transformers

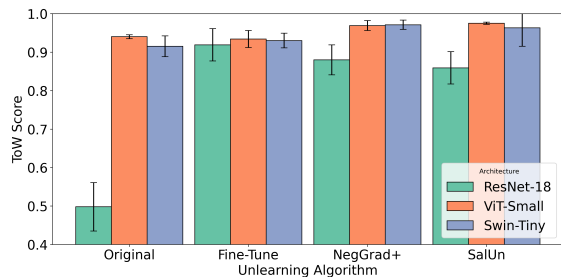
Table 12. Comparison of vanilla and RUM-integrated unlearning methods on CIFAR-100. Results are reported using ToW and ToW-MIA (higher is better). Best results in each row are shown in bold.

Method	Within RUM		Vanilla (w/o RUM)	
	ToW $\uparrow$	ToW-MIA $\uparrow$	ToW $\uparrow$	ToW-MIA $\uparrow$
Original	0.619	0.538	Same as left	
Fine-tune	<b>0.855</b>	<b>0.889</b>	0.807	0.844
NegGrad+	<b>0.931</b>	0.838	0.888	<b>0.845</b>
SalUn	<b>0.903</b>	<b>0.709</b>	0.884	0.686

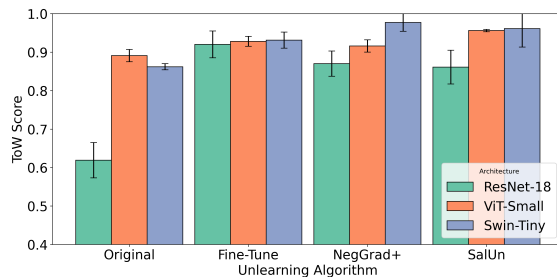
(a) ViT-Small

Method	Within RUM		Vanilla (No RUM)	
	ToW $\uparrow$	ToW-MIA $\uparrow$	ToW $\uparrow$	ToW-MIA $\uparrow$
Original	0.670	0.586	Same as left	
Fine-tune	<b>0.822</b>	<b>0.839</b>	0.774	0.781
NegGrad+	<b>0.975</b>	<b>0.902</b>	0.851	0.831
SalUn	<b>0.870</b>	<b>0.751</b>	0.833	0.640

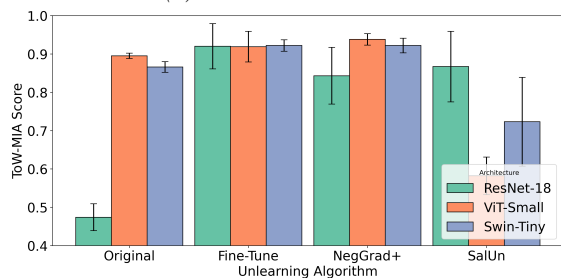
(b) Swin-Tiny



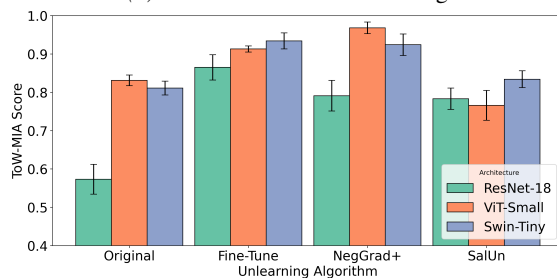
(a) ToW with Confidence



(b) ToW with Holdout Retraining



(c) ToW-MIA with Confidence



(d) ToW-MIA with Holdout Retraining

Figure 5. Architecture performance comparison on CIFAR-10

the Holdout Retraining proxy.

### A.8. Results for SVHN

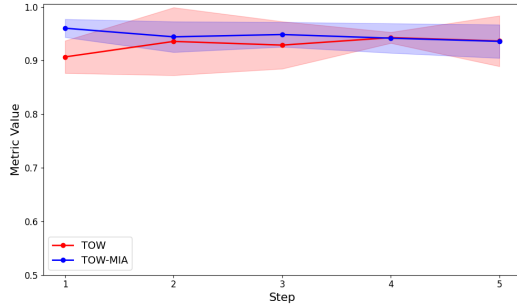
#### A.8.1. DETAILED ToW AND ToW-MIA RESULTS ACROSS VTs FOR SVHN

To extend our study to a different dataset, we repeat the experiments on SVHN using both ViT-Small and Swin-Tiny architectures. Table 18 lists the hyperparameter settings used for the original model training and subsequent retraining.

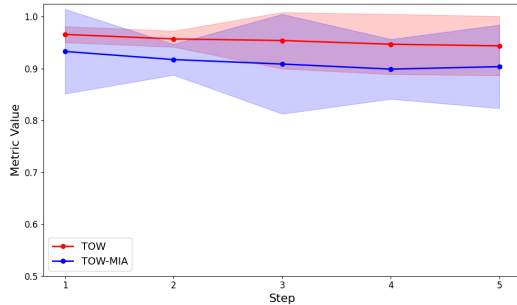
Table 18. Training configurations and hyperparameters used for original models  $\theta_o$  and retrained models  $\theta_r$  alike, using ViT-Small and Swin-Tiny architectures on the SVHN dataset.

Hyperparameter	ViT-Small	Swin-Tiny
<b>Optimizer</b>	AdamW	AdamW
<b>Base learning rate</b>	0.0001	0.0001
<b>Loss</b>	Cross-Entropy	Cross-Entropy
<b>Learning rate scheduler</b>	CosineAnnealingLR	CosineAnnealingLR
<b>Batch size</b>	256	256
<b>Epochs</b>	30	30
<b>Weight decay</b>	0.01	0.05
<b>Data augmentation</b>	-	-

Following the procedure in Section 4.2, we apply all unlearn methods within the  $RUM_F$  meta-algorithm to the SVHN dataset. We evaluate both ViT-Small and Swin-Tiny architectures, using Confidence and Holdout Retraining as proxy metrics. Figure 7 shows the comparative unlearning performance of these methods on SVHN. See Section 4.2 for a detailed discussion of the results.



(a) ViT-Small



(b) Swin-Tiny

Figure 6. Continual Unlearning Performance Across Multiple Steps on CIFAR-10.

### A.8.2. CONTINUAL UNLEARNING RESULTS IN VTs FOR SVHN

We follow the same procedure outlined in Section 4.5 to sequentially apply NegGrad+ and Holdout Retraining on the SVHN dataset over five consecutive steps. The results are presented in Figure 8, evaluated by ToW and ToW-MIA. They further support the observation from Section 4.5: continual unlearning in VTs exhibits high stability across steps, with minimal degradation in performance.

Table 13. Detailed performance results for the two VTs across both the CIFAR datasets.

Algorithm	Confidence		Holdout Ret	
	ToW ( $\uparrow$ )	ToW-MIA ( $\uparrow$ )	ToW ( $\uparrow$ )	ToW-MIA ( $\uparrow$ )
Original	$0.940 \pm 0.005$	$0.895 \pm 0.007$	$0.891 \pm 0.016$	$0.831 \pm 0.014$
Fine-tune	$0.934 \pm 0.022$	$0.919 \pm 0.040$	$0.928 \pm 0.013$	$0.913 \pm 0.008$
NegGrad+	$0.969 \pm 0.013$	$0.938 \pm 0.015$	$0.916 \pm 0.016$	$0.968 \pm 0.015$
SalUn	$0.975 \pm 0.003$	$0.582 \pm 0.049$	$0.956 \pm 0.003$	$0.766 \pm 0.039$

(a) CIFAR-10 – ViT-Small

Algorithm	Confidence		Holdout Ret	
	ToW ( $\uparrow$ )	ToW-MIA ( $\uparrow$ )	ToW ( $\uparrow$ )	ToW-MIA ( $\uparrow$ )
Original	$0.915 \pm 0.027$	$0.866 \pm 0.014$	$0.862 \pm 0.008$	$0.811 \pm 0.018$
Fine-tune	$0.930 \pm 0.019$	$0.922 \pm 0.015$	$0.923 \pm 0.021$	$0.931 \pm 0.021$
NegGrad+	$0.971 \pm 0.012$	$0.922 \pm 0.019$	$0.977 \pm 0.023$	$0.924 \pm 0.028$
SalUn	$0.963 \pm 0.048$	$0.723 \pm 0.116$	$0.961 \pm 0.048$	$0.834 \pm 0.022$

(b) CIFAR-10 – Swin-Tiny

Algorithm	Confidence		Holdout Ret	
	ToW ( $\uparrow$ )	ToW-MIA ( $\uparrow$ )	ToW ( $\uparrow$ )	ToW-MIA ( $\uparrow$ )
Original	$0.629 \pm 0.038$	$0.521 \pm 0.026$	$0.619 \pm 0.040$	$0.538 \pm 0.023$
Fine-tune	$0.813 \pm 0.008$	$0.831 \pm 0.014$	$0.855 \pm 0.036$	$0.889 \pm 0.008$
NegGrad+	$0.844 \pm 0.034$	$0.736 \pm 0.023$	$0.931 \pm 0.039$	$0.838 \pm 0.024$
SalUn	$0.923 \pm 0.019$	$0.602 \pm 0.014$	$0.903 \pm 0.049$	$0.709 \pm 0.085$

(c) CIFAR-100 – ViT-Small

Algorithm	Confidence		Holdout Ret	
	ToW ( $\uparrow$ )	ToW-MIA ( $\uparrow$ )	ToW ( $\uparrow$ )	ToW-MIA ( $\uparrow$ )
Original	$0.665 \pm 0.014$	$0.553 \pm 0.015$	$0.670 \pm 0.027$	$0.586 \pm 0.025$
Fine-tune	$0.774 \pm 0.030$	$0.758 \pm 0.015$	$0.822 \pm 0.034$	$0.839 \pm 0.032$
NegGrad+	$0.867 \pm 0.021$	$0.767 \pm 0.019$	$0.975 \pm 0.027$	$0.902 \pm 0.035$
SalUn	$0.835 \pm 0.060$	$0.557 \pm 0.034$	$0.870 \pm 0.039$	$0.751 \pm 0.043$

(d) CIFAR-100 – Swin-Tiny

Table 14. Detailed performance result metrics for ResNet-18 and ResNet-50 on the CIFAR-10 and CIFAR-100 datasets respectively.

Algorithm	Confidence		Holdout Retraining	
	ToW ( $\uparrow$ )	ToW-MIA ( $\uparrow$ )	ToW ( $\uparrow$ )	ToW-MIA ( $\uparrow$ )
Fine-tune	$0.919 \pm 0.042$	$0.920 \pm 0.059$	$0.920 \pm 0.035$	$0.865 \pm 0.033$
NegGrad+	$0.880 \pm 0.039$	$0.843 \pm 0.074$	$0.870 \pm 0.033$	$0.791 \pm 0.040$
SalUn	$0.859 \pm 0.042$	$0.867 \pm 0.092$	$0.861 \pm 0.044$	$0.783 \pm 0.028$

(a) CIFAR-10 with ResNet-18

Algorithm	Confidence		Holdout Retraining	
	ToW ( $\uparrow$ )	ToW-MIA ( $\uparrow$ )	ToW ( $\uparrow$ )	ToW-MIA ( $\uparrow$ )
Fine-tune	$0.863 \pm 0.049$	$0.857 \pm 0.059$	$0.846 \pm 0.032$	$0.792 \pm 0.044$
NegGrad+	$0.890 \pm 0.047$	$0.922 \pm 0.017$	$0.866 \pm 0.031$	$0.838 \pm 0.027$
SalUn	$0.665 \pm 0.031$	$0.636 \pm 0.038$	$0.696 \pm 0.032$	$0.699 \pm 0.034$

(b) CIFAR-100 with ResNet-50

**Benchmarking Unlearning for Vision Transformers**

Table 15. Accuracies on  $D_r$ ,  $D_f$  and  $D_{test}$  for the ‘‘Retrain’’ models  $\theta_r$ , as well as the respective ‘‘Unlearned’’ models  $\theta_u$ , evaluated across all unlearning algorithms within the RUM<sub>F</sub> framework. MIA performance is also reported. Results are averaged over 3 runs, with 95% confidence intervals.

Algorithm	Confidence				Holdout Retaining			
	Retain Acc	Forget Acc	Test Acc	MIA	Retain Acc	Forget Acc	Test Acc	MIA
Retrain	99.969 ± 0.006	94.089 ± 0.456	93.703 ± 0.486	0.108 ± 0.007	99.974 ± 0.035	89.244 ± 1.321	93.767 ± 0.029	0.174 ± 0.012
Fine-tune	99.433 ± 0.639	94.111 ± 0.912	87.947 ± 1.519	0.128 ± 0.014	99.562 ± 0.347	87.889 ± 2.356	88.240 ± 0.348	0.204 ± 0.016
NegGrad+	99.832 ± 0.140	93.411 ± 1.078	91.407 ± 0.872	0.069 ± 0.008	99.814 ± 0.073	83.289 ± 2.115	91.340 ± 0.413	0.167 ± 0.020
SalUn	100.000 ± 0.000	96.033 ± 0.543	93.203 ± 0.617	0.523 ± 0.057	100.000 ± 0.000	93.089 ± 1.971	93.180 ± 0.523	0.403 ± 0.042

(a) CIFAR-10 with ViT-Small

Algorithm	Confidence				Holdout Retaining			
	Retain Acc	Forget Acc	Test Acc	MIA	Retain Acc	Forget Acc	Test Acc	MIA
Retrain	99.961 ± 0.021	91.867 ± 1.711	91.607 ± 0.596	0.133 ± 0.002	99.979 ± 0.027	86.389 ± 1.246	91.767 ± 0.689	0.190 ± 0.020
Fine-tune	99.833 ± 0.141	96.733 ± 0.840	89.463 ± 0.660	0.076 ± 0.005	99.779 ± 0.012	91.478 ± 0.208	89.183 ± 0.352	0.148 ± 0.009
NegGrad+	99.968 ± 0.018	93.833 ± 0.597	90.643 ± 1.096	0.064 ± 0.005	99.903 ± 0.024	81.911 ± 0.694	90.473 ± 0.254	0.181 ± 0.007
SalUn	100.000 ± 0.000	93.967 ± 8.103	90.743 ± 0.547	0.403 ± 0.126	100.000 ± 0.000	88.533 ± 9.399	91.160 ± 0.692	0.351 ± 0.043

(b) CIFAR-10 with Swin-Tiny

Algorithm	Confidence				Holdout Retaining			
	Retain Acc	Forget Acc	Test Acc	MIA	Retain Acc	Forget Acc	Test Acc	MIA
Retrain	98.457 ± 0.819	69.322 ± 1.788	69.670 ± 2.445	0.432 ± 0.012	98.063 ± 0.413	68.767 ± 3.828	69.467 ± 1.032	0.412 ± 0.024.
Fine-tune	99.325 ± 0.148	86.056 ± 1.907	68.193 ± 1.578	0.283 ± 0.014	99.322 ± 0.622	81.200 ± 2.766	68.350 ± 1.433	0.322 ± 0.025
NegGrad+	99.846 ± 0.166	82.200 ± 0.299	71.440 ± 1.793	0.192 ± 0.004	99.637 ± 0.177	72.722 ± 0.621	70.997 ± 0.448	0.276 ± 0.006
SalUn	99.982 ± 0.007	64.756 ± 0.669	71.467 ± 0.816	0.810 ± 0.014	99.981 ± 0.006	63.878 ± 2.161	72.620 ± 0.480	0.666 ± 0.068

(c) CIFAR-100 with ViT-Small

Algorithm	Confidence				Holdout Retaining			
	Retain Acc	Forget Acc	Test Acc	MIA	Retain Acc	Forget Acc	Test Acc	MIA
Retrain	99.220 ± 0.167	69.833 ± 1.242	68.923 ± 0.296	0.430 ± 0.015	99.143 ± 0.185	70.267 ± 2.848	69.057 ± 0.827	0.392 ± 0.024
Fine-tune	99.638 ± 0.184	91.811 ± 3.019	68.503 ± 0.405	0.194 ± 0.022	99.368 ± 0.557	87.289 ± 1.300	68.377 ± 1.536	0.239 ± 0.016
NegGrad+	99.940 ± 0.047	81.900 ± 0.955	69.410 ± 1.083	0.207 ± 0.002	99.914 ± 0.047	70.111 ± 0.723	69.833 ± 0.521	0.308 ± 0.009
SalUn	99.965 ± 0.003	55.578 ± 6.181	70.750 ± 0.676	0.859 ± 0.054	99.966 ± 0.007	60.156 ± 1.615	71.490 ± 0.696	0.616 ± 0.021

(d) CIFAR-100 with Swin-Tiny

Table 16. Detailed unlearning performance at each of the 5 sequential steps for the NegGrad+ and Holdout Retraining configuration discussed in Section 4.5 and displayed in Figures 2 and 6.

Step	CIFAR-10				CIFAR-100			
	ViT-Small		Swin-Tiny		ViT-Small		Swin-Tiny	
	ToW (↑)	ToW-MIA (↑)						
1	0.907 ± 0.030	0.960 ± 0.017	0.966 ± 0.016	0.933 ± 0.082	0.891 ± 0.065	0.816 ± 0.051	0.906 ± 0.039	0.823 ± 0.023
2	0.936 ± 0.063	0.944 ± 0.029	0.957 ± 0.016	0.917 ± 0.030	0.868 ± 0.031	0.770 ± 0.015	0.840 ± 0.064	0.764 ± 0.085
3	0.929 ± 0.044	0.948 ± 0.023	0.954 ± 0.054	0.909 ± 0.096	0.857 ± 0.049	0.764 ± 0.047	0.853 ± 0.052	0.776 ± 0.055
4	0.943 ± 0.010	0.942 ± 0.028	0.947 ± 0.058	0.899 ± 0.058	0.858 ± 0.053	0.760 ± 0.040	0.843 ± 0.021	0.746 ± 0.035
5	0.936 ± 0.047	0.936 ± 0.031	0.944 ± 0.057	0.904 ± 0.080	0.851 ± 0.006	0.754 ± 0.056	0.870 ± 0.070	0.781 ± 0.089

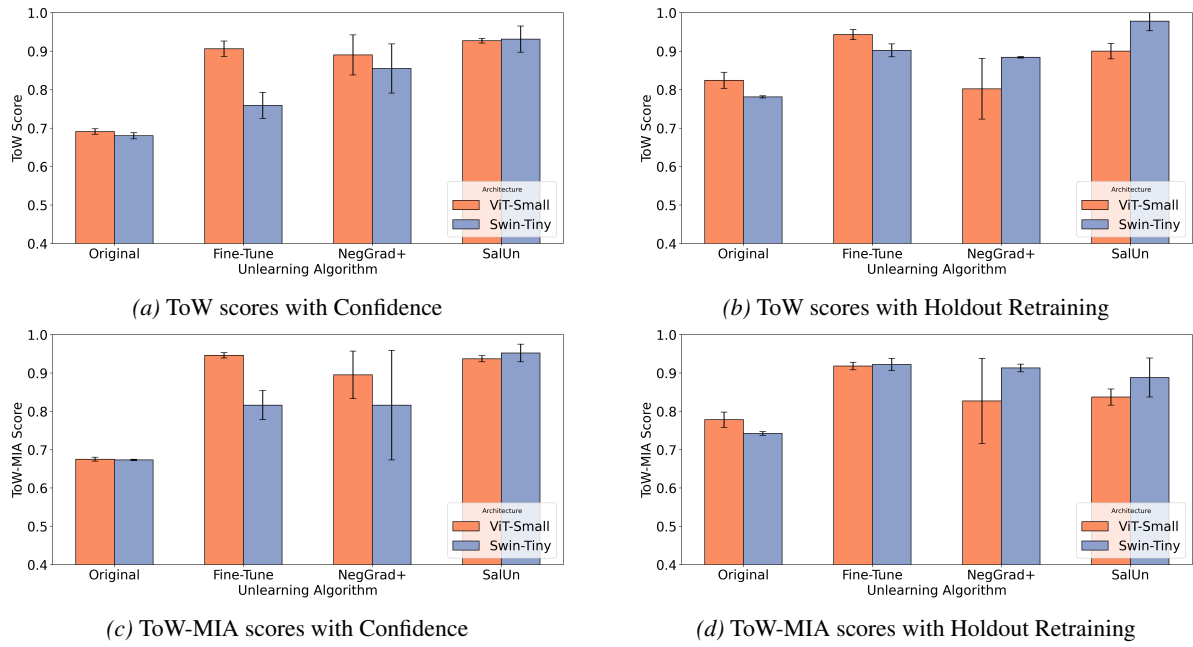
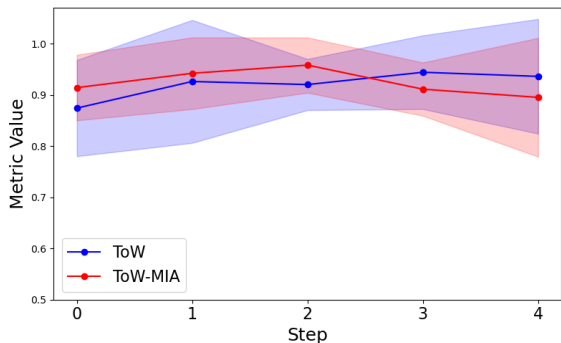


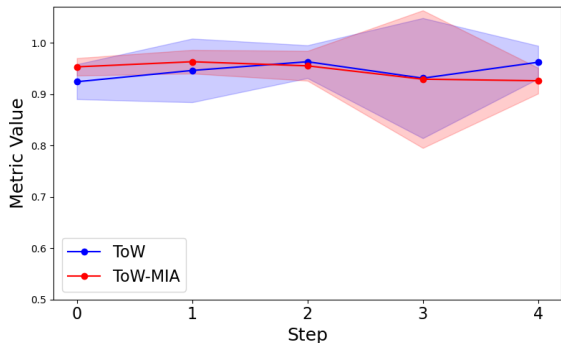
Figure 7. MU performance comparison on SVHN

Table 17. Continual unlearning over 10 sequential steps on CIFAR-100 using NegGrad+ with the Holdout Retraining proxy (configuration discussed in Section 4.5). Results are reported as mean  $\pm$  95% confidence interval.

Step	ViT-Small		Swin-Tiny	
	ToW ( $\uparrow$ )	ToW-MIA ( $\uparrow$ )	ToW ( $\uparrow$ )	ToW-MIA ( $\uparrow$ )
1	0.947 $\pm$ 0.043	0.889 $\pm$ 0.108	0.947 $\pm$ 0.035	0.860 $\pm$ 0.082
2	0.971 $\pm$ 0.033	0.828 $\pm$ 0.040	0.900 $\pm$ 0.104	0.786 $\pm$ 0.064
3	0.973 $\pm$ 0.019	0.845 $\pm$ 0.034	0.953 $\pm$ 0.021	0.850 $\pm$ 0.024
4	0.918 $\pm$ 0.053	0.840 $\pm$ 0.244	0.940 $\pm$ 0.081	0.816 $\pm$ 0.094
5	0.921 $\pm$ 0.046	0.769 $\pm$ 0.020	0.958 $\pm$ 0.079	0.834 $\pm$ 0.138
6	0.966 $\pm$ 0.029	0.807 $\pm$ 0.129	0.921 $\pm$ 0.059	0.817 $\pm$ 0.025
7	0.951 $\pm$ 0.040	0.841 $\pm$ 0.108	0.908 $\pm$ 0.062	0.792 $\pm$ 0.111
8	0.961 $\pm$ 0.024	0.817 $\pm$ 0.046	0.939 $\pm$ 0.041	0.798 $\pm$ 0.126
9	0.946 $\pm$ 0.049	0.807 $\pm$ 0.068	0.936 $\pm$ 0.054	0.822 $\pm$ 0.089
10	0.923 $\pm$ 0.080	0.825 $\pm$ 0.115	0.921 $\pm$ 0.072	0.803 $\pm$ 0.100



(a) ViT-Small



(b) Swin-Tiny

Figure 8. Continual Unlearning Performance Across Five Steps on SVHN